Journal of Structural Geology, Vol. 7, No. 5, pp. 513 to 525, 1985
Printed in Great Britain

0191-8141/85 $03.00 + 0.00

Ductile-to-brittle transition in shear during thrust sheet emplacement, Southern Appalachian thrust belt

R. G. GIBSON

Department of Geological Sciences, Virginia Polytechnic Institute, Blacksburg, VA 24061, U.S.A.

and

D. R. GRAY

Department of Earth Sciences, Monash University, Clayton, Victoria 3168, Australia

(*Received* 3 *January* 1984; *accepted in revised form* 25 *September* 1984)

Abstract—Mesoscopic structures in anchimetamorphic (T = 200–300°C) strata of the Pulaski thrust sheet, Southern Appalachian thrust belt, developed in progressive, heterogeneous simple shear near the ductile-to-brittle transition. Shear ($\gamma \leq 3$) was localized in weak, anisotropic pelitic rocks (Rome Formation) along the base of this 5–11 km thick thrust sheet. Folds, which vary from upright and open to isoclinal and NW-facing, developed during ductile shearing and display a correlation between tightness and axial-surface dip. Movement along brecciated thrust zones, which evolved progressively from zones of greatest ductile strain, resulted in low-angle truncation of fold axis trends, coaxial refolding of earlier structures, and imbrication of the thrust sheet.

Transient variations in fluid pressure (P_f) controlled the mechanical behavior of the thrust sheet. Systematic veins imply $P_f > \sigma_3 + T$ (T = tensile strength) during ductile deformation, whereas later non-systematic vein arrays in high strain zones record periods of nearly hydrostatic stress. Elevated P_f, which led to fracturing, dilation, and fault initiation, appears confined to pelitic zones within the Rome Formation. This, coupled with decreasing temperature, resulted in the transition from ductile folding to brittle thrusting. Changing physical conditions probably reflect erosional unroofing during uplift and late Paleozoic thrust sheet emplacement.

INTRODUCTION

LOW-ANGLE thrust faulting is known to be the major shortening mechanism in many deformed fold-and-thrust belts (Gwinn 1964, Bally *et al.* 1966, Suppe 1980, Boyer & Elliott 1982). Nonetheless, internal portions of such belts commonly display a significant component of ductile strain even at conditions below greenschist grade (Schmid 1975, Beach 1981, Ramsay *et al.* 1983). Likewise, strata within individual thrust sheets may display contrasting mechanical behavior related to position within the sheet (Elliott 1976, Sanderson 1982, Wojtal 1982). This variable response of rocks to deformation has been treated as the transition from infra- to suprastructure (DeSitter & Zwart 1960, Fyson 1971) or ductile to brittle regimes (Beach 1981) and probably reflects physical conditions during deformation.

In this paper, the ductile-to-brittle transition is discussed with regard to deformation of the Lower Cambrian Rome Formation in the Pulaski thrust sheet of the Southern Appalachian thrust belt. Mesoscopic and microscopic analysis of selected outcrops throughout the study area (Figs. 1a & b) has enabled correlation of mechanical behavior with changing physical conditions. New data, together with previously published work, is integrated into a regional model for thrust sheet evolution.

GEOLOGIC SETTING

The Southern Appalachian fold-and-thrust belt (Valley and Ridge Province, Fig. 1a) consists of deformed Paleozoic sedimentary rocks that were transported northwestward on stair-stepped, southeast-dipping thrusts that merge into a master décollement horizon (Gwinn 1964, Harris & Milici 1977). It is bound on the southeast by allochthonous metamorphic rocks of the Blue Ridge Province (Harris & Bayer 1979, Cook *et al.* 1979).

The Pulaski thrust extends approximately 500 km along strike and is the most southeasterly of four major thrusts in the southwest Virginia thrust belt. It places dominantly Cambro-Ordovician rocks on Ordovician to Mississippian strata of the Saltville thrust sheet and has an estimated horizontal displacement of 15–50 km (Cooper 1970, Bartholomew 1979). In the study area, the Pulaski thrust sheet consists of a northwestern belt of Middle Cambrian and younger carbonates and a southeastern belt of Lower Cambrian Rome Formation (Fig. 1b). The Rome Formation is comprised of interbedded to interlaminated mudstone, siltstone, sandstone, and microcrystalline dolomite (Spigai 1963) gradational into competent, thick-bedded dolomites (Shady Formation) below and cyclic carbonates (Elbrook Formation) above (Fig. 2). The Rome–Elbrook contact occurs within a transitional interval of argillaceous carbonates and is faulted along the Max Meadows thrust (Fig. 1b) (Cooper 1939, Schultz 1983).

In the Blacksburg–Pulaski area, the Pulaski thrust system, including the Max Meadows thrust, is an imbricate fan (Fig. 1c). It is not known whether the imbricates within the Pulaski sheet were 'blind' (Boyer & Elliott

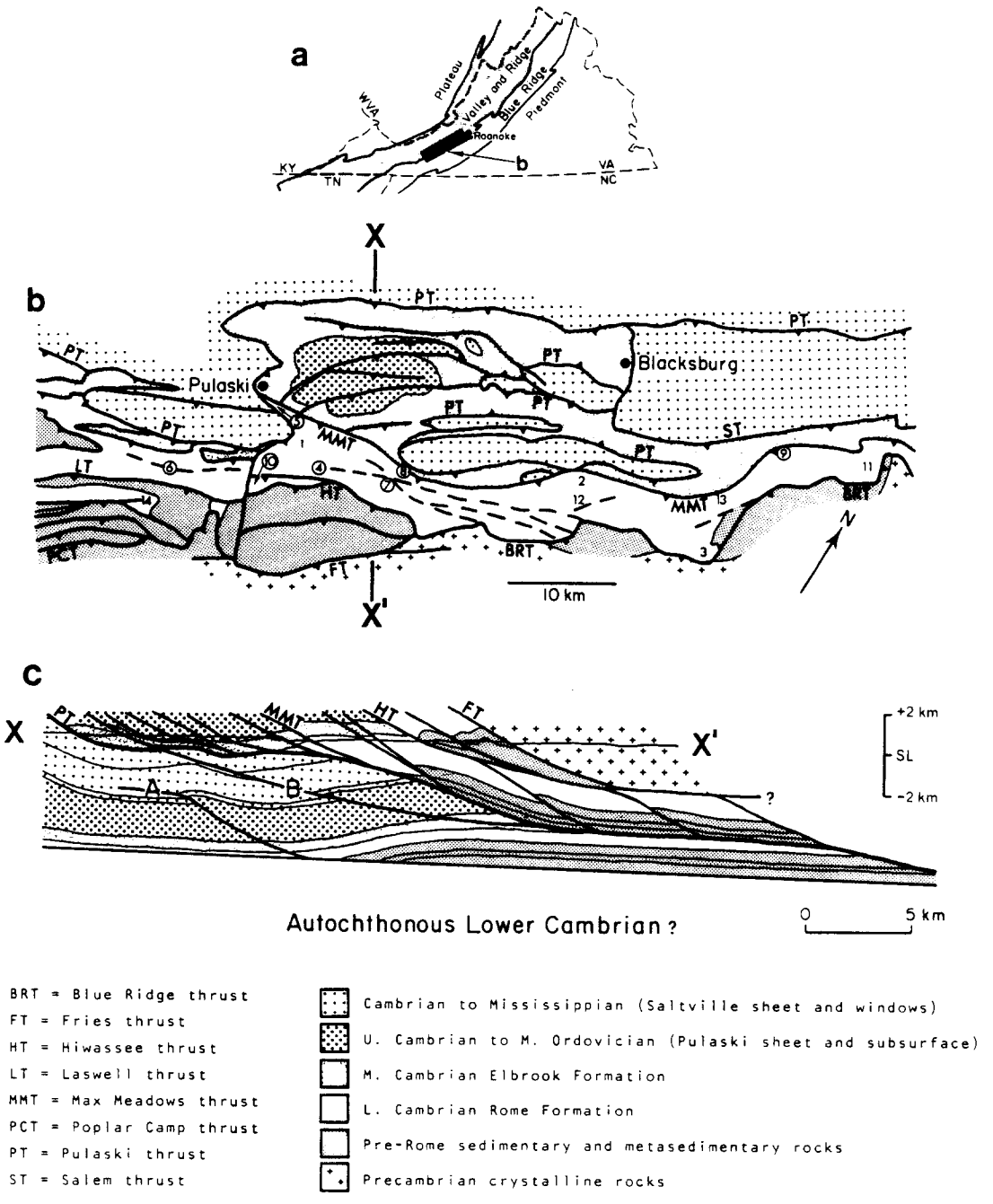

Fig. 1. (a) Geologic provinces of the Appalachians in Virginia (VA) showing location of fold-and-thrust belt (shaded) and Fig. 1b. (b) Map of Pulaski thrust sheet and adjacent areas after Cooper (1939), Stose & Stose (1957), Bartholomew *et al.* (1980) and Schultz (in press). Dashed lines are inferred fault traces (Gibson 1983). Numbers are outcrop locations cited in text; circles indicate inclined folds. (c) Interpretive cross-section X–X′ across the Pulaski–Blue Ridge thrust system drawn assuming that fault A predates B (chronology after Schultz 1983) and Rome Formation in Pulaski sheet is tectonically thickened (Wells 1975). Shortening across the Pulaski thrust and its imbricates totals approximately 35 km.

1982) or merged upward with the Blue Ridge thrust system. The Blue Ridge, Hiwassee, and Laswell thrusts (Fig. 1b) define the base of the Blue Ridge sheet and, possibly, the roof of a duplex floored by the Pulaski thrust (Fig. 1c) (cf. Boyer & Elliott 1982).

The Pulaski sheet is structurally more complex than other thrust sheets in this part of the Appalachians. Folding of the Pulaski thrust, indicated by numerous erosional windows between Pulaski and Blacksburg (Fig. 1b), probably reflects incorporation of horses into the sole of the sheet. These horses were derived from the Cambrian to Mississippian footwall ramp (Fig. 1c) (Bartholomew *et al.* 1980, 1982, Schultz 1979, 1983, in press). A 500 m thick broken formation zone, consisting of variably oriented folds in a matrix of tectonic breccia, occurs within the upper Rome and lower Elbrook Formations along the base of the Pulaski sheet northwest of the Max Meadows thrust (Cooper & Haff 1940, Cooper 1970, Schultz 1983, in press). Upper Elbrook carbonates, structurally above the broken formation zone, display only minor mesoscopic deformation (Schultz 1983, in press).

Conodont color-alteration data yield maximum paleotemperatures of 200–300°C (CAI = 4–5) in the

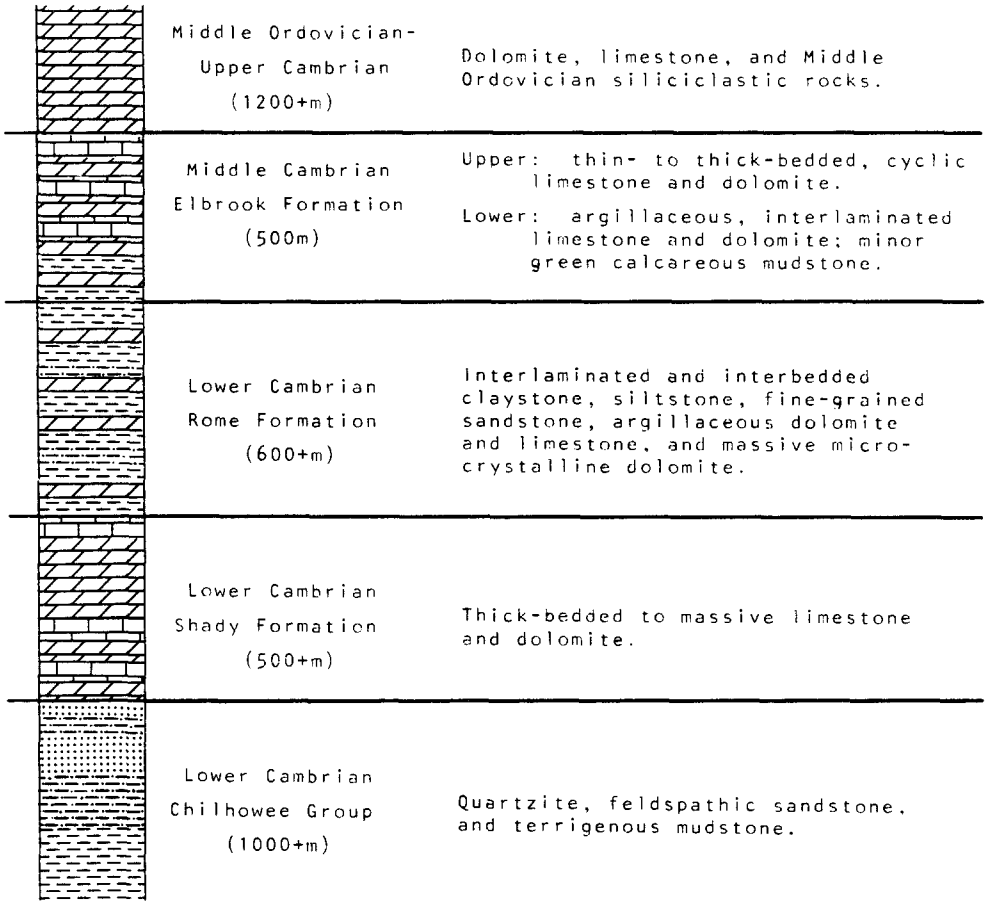

Fig. 2. Simplified stratigraphic column for the Pulaski thrust sheet.

Pulaski sheet (Epstein *et al.* 1977). Illite crystallinity values from the Elbrook Formation are consistent with these anchimetamorphic temperatures (Schultz in press, Schweitzer 1984). Inferred temperatures for more westerly thrust sheets are considerably lower (Epstein *et al.* 1977).

The present study area consists of the outcrop belt of the Rome Formation southeast of the Max Meadows thrust (Fig. 1b). Due to lack of stratigraphic control, large scale structures within the Max Meadows sheet have not yet been defined by surface mapping. However, analysis of aerial photographs indicates a lack of macroscopic folds and shows that mesoscopic fold axis trends are truncated by both the Max Meadows and Blue Ridge thrusts, as well as by several inferred thrust faults within the sheet (Fig. 1b) (Gibson 1983).

STRUCTURAL FEATURES

Max Meadows sheet

Mesoscopic folding and faulting account for much of the strain within the Max Meadows sheet. Deformational style, reflected largely by fold attitude, varies between and within individual outcrops. Structures are discussed in terms of two end-member associations.

Zones of upright folds. Structures of this domain occur in relatively competent strata, including siltstone, sandstone, and thick-bedded dolomite. Mesoscopic folds are tight to open, symmetric to slightly NW-verging, and have steeply dipping axial surfaces (Fig. 6a). Fold axes lie in the NE and SW quadrants, depending on location within the thrust sheet, and plunge gently in either direction (Figs. 3a & b). Axial orientations cluster tightly (Fig. 3a) or show marked plunge variation within a single outcrop (Fig. 3b). Strata face upward in all upright fold domains.

Contraction faults, typically marked by breccia zones 1–10 cm thick, occur mainly near the Max Meadows or Blue Ridge thrusts and are rare in the internal portions of the sheet. They dip moderately to steeply SE and are always at a low angle to bedding. Slickensides are conspicuously absent from both bedding and contraction fault surfaces. Mineral veins are uncommon and largely restricted to fold closures and near minor faults.

Zones of inclined folds. Transitional with zones of upright folds are regions characterized by moderately inclined, strongly asymmetric, tight to isoclinal folds with SE-dipping axial surfaces. Such folds are localized in sections dominated by mudstone and argillaceous carbonate, especially where adjacent to the Max Meadows thrust or inferred faults within the sheet (locs. 4–10, Fig. 1b). The transition from upright to inclined folds involves decreasing axial plane dip accompanied by decreasing fold interlimb angle (Fig. 4), increased fracturing and veining, appearance of boudinaged bedding, and increased number and closer spacing of breccia horizons and contraction faults.

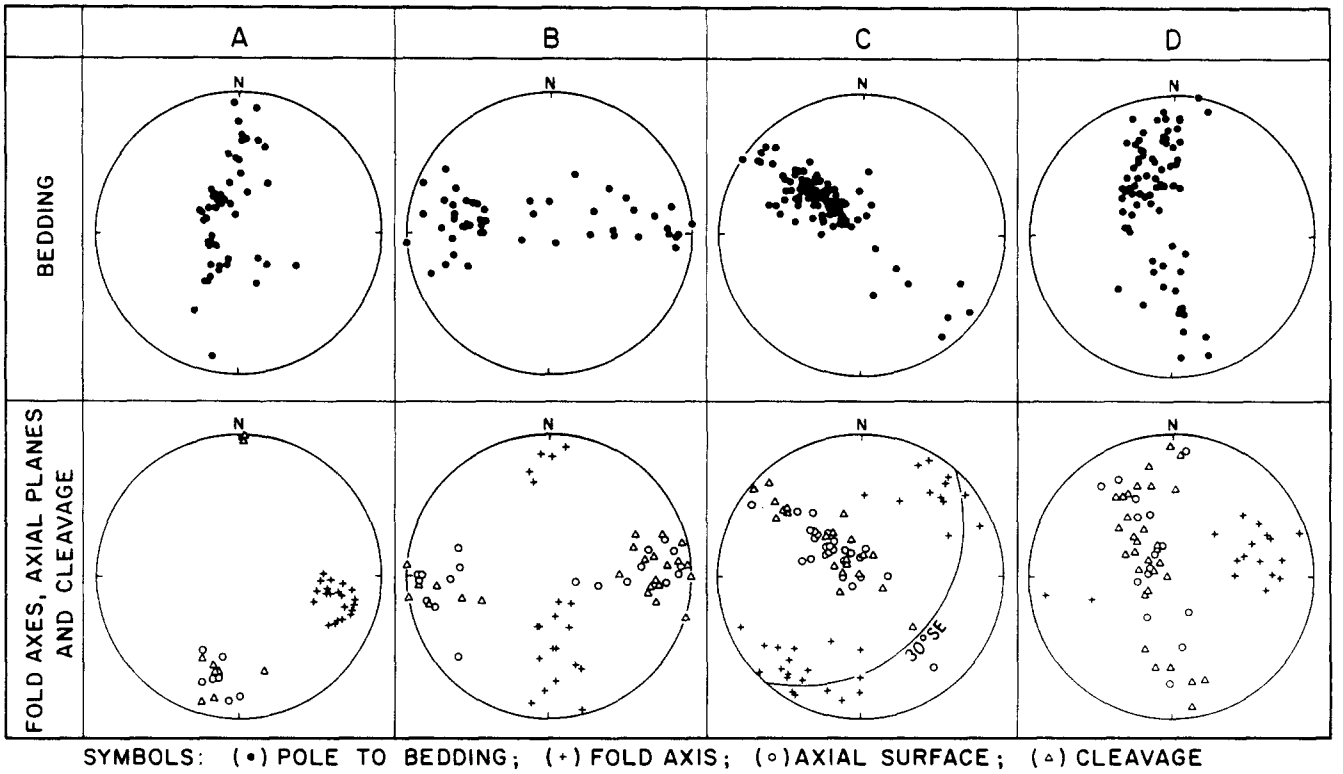

Fig. 3. Field orientation data from representative outcrops. (a) Upright fold zone, loc. 2 (Fig. 1b) (n = 49 S_o, 21 *F.A.*, 7 *A.S.*, 7 *Cl.*). (b) Upright fold zone, loc. 3 (Fig. 1b) (n = 51 S_o, 20 *F.A.*, 19 *A.S.*, 24 *Cl.*). (c) Inclined fold zone, loc. 4 (Fig. 1b) (n = 92 S_o, 31 *F.A.*, 26 *A.S.*, 21 *Cl.*). (d) Upright and inclined folds, loc. 11 (Fig. 1b) (n = 77 S_o, 17 *F.A.*, 15 *A.S.*, 31 *Cl.*).

Fold axes plunge gently NE or SW and often display considerable scatter (Fig. 3c). Minor fold axes from a wide belt of inclined folds (loc. 4, Fig. 1b) define a crude partial girdle, dipping 20–30° SE and coinciding with the average axial surface orientation for mesoscopic folds within the outcrop (Fig. 3c). Gently curved (less than 45°) minor fold hinges are uncommon. Axial surfaces vary in dip from vertical to nearly horizontal (Figs. 3c & d) and are locally curved (e.g. SE end of section in Fig. 5). The folds have complex geometries with fold form varying between adjacent lithologies and along individual layers (Fig. 5b). Mesoscopic fold closures are commonly polyclinal and cm-scale, disharmonic, parasitic folds in interlaminated lithologies account for thickening in fold hinges (Fig. 5a).

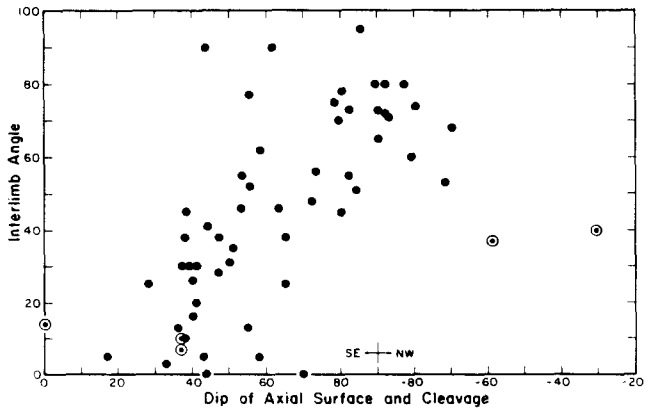

Fig. 4. Graph of mesoscopic fold interlimb angle vs.axial surface/cleavage dip (n = 59). Open circles indicate outcrops affected by refolding.

Contraction faults dip moderately SE and are either parallel to bedding or truncate it at a low angle. Breccia zones, up to several m thick, characterize most fault surfaces and locally separate slices of non-brecciated rock less than 1 m thick (Fig. 6b). Layers adjacent to breccia horizons contain abundant asymmetric cm-scale folds, display a phyllitic fabric, and are intensely veined (Fig. 6c).

Boudins, ranging up to several m long, consist of intensely veined dolomite or red mudstone. Near the Max Meadows thrust (loc. 5, Fig. 1b), isolated fold hinges of thin-bedded dolomite occur in a cleaved carbonate matrix (Fig. 6d). In other outcrops (loc. 4, Fig. 1b), boudin-shaped dolomite blocks rest in a poorly-foliated carbonate breccia (Fig. 5c) and distinct microcrystalline dolomite laminae are separated obliquely across carbonate-filled voids on the limbs of isoclinal folds (Fig. 6f). Pinch-and-swell structures (internal boudins of Cobbold *et al.* 1971) on fold limbs (Fig. 6e) are gradational into intensely veined, brittle shear zones with extensional offset. Planar and en-echelon veins are abundant and best developed in thick-bedded dolomite, non-laminated mudstone, the cores of isoclinal folds (Fig. 5a), and in contorted strata bounding breccia zones (Fig. 6c).

Second generation structures. On the basis of locally refolded folds, regional fanning of axial surfaces (e.g. Fig. 3d), and fold-thrust relationships, earlier workers (Bartholomew & Lowry 1979, Bartholomew *et al.* 1980, 1982) considered much of the Pulaski thrust sheet

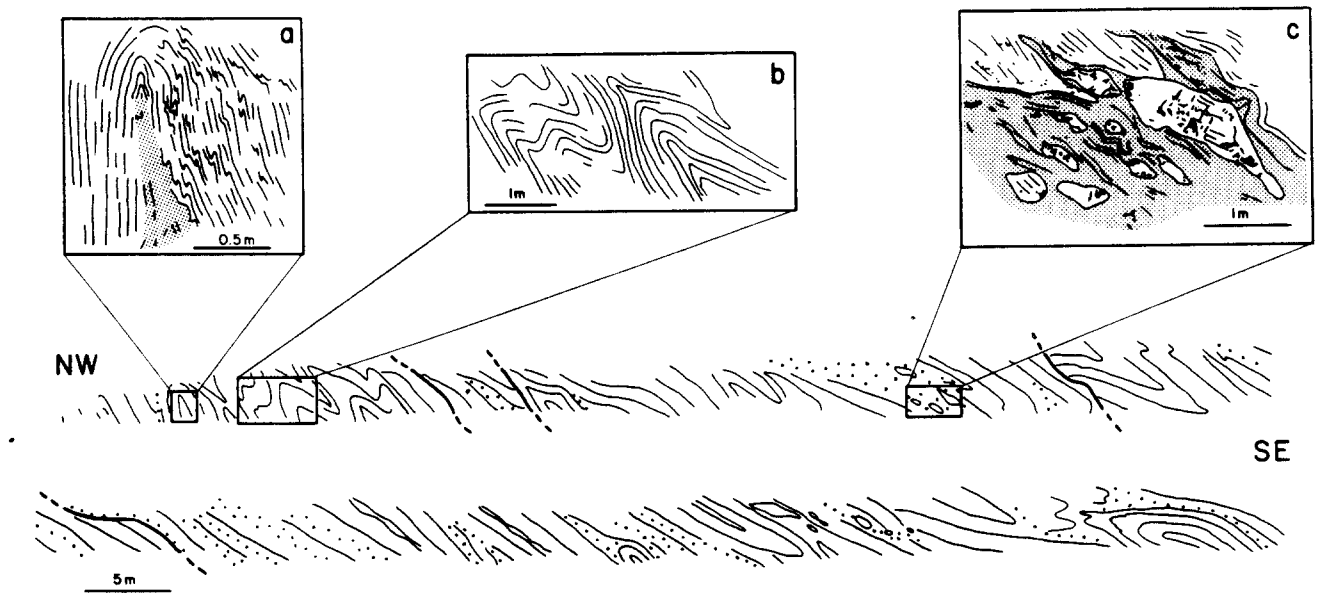

Fig. 5. Outcrop section of inclined folds, loc. 4 (Fig. 1b). Form lines, bedding; dots, breccias. (a) Fold in interlaminated dolomite and mudstone showing parasitic folds and fracturing in core (shaded). (b) Variable fold form in red mudstones. (c) Intensely veined (black) dolomite boudins in poorly foliated breccia (shaded).

polydeformed. Structures that deform earlier folds or a tectonic fabric occur sporadically throughout the Max Meadows sheet though they are localized within or near zones of inclined folds and faults. Most outcrops show no evidence of polyphase deformation.

Second-generation fold axes, crenulation axes, and bedding–crenulation intersection lineations plunge gently NE or SW and axial surfaces dip gently to moderately SE. Refolding of pre-existing folds is coaxial (Fig. 7) and often localized along minor faults (Fig. 6g). Second-generation crenulation cleavages occur at angles from 30 to 90° to fault zones. Clasts within the breccia zones frequently contain at least one crenulation of a pre-existing tectonic foliation (Gibson 1983).

Blue Ridge sheet

The Blue Ridge thrust system varies along its length from a single discontinuity in the northeast to an imbricate thrust complex in the southwest (Fig. 1b). Precambrian granulite gneisses and greenschist-grade metasediments comprise the Blue Ridge sheet adjacent to the northeastern part of the study area (Bartholomew *et al.* 1982). Where the Blue Ridge thrust branches into several imbricates toward the southwest, unmetamorphosed Lower Cambrian sedimentary rocks comprise the hanging wall.

The Laswell and Hiwassee thrusts define the front of the Blue Ridge thrust system along its southwestern extent (McDowell 1968). Northwest of these faults, the Shady Formation grades upward through a sequence of argillaceous carbonates into red mudstones of the basal Rome. Breccia zones and minor folds with variably oriented axial surfaces are abundant within this transitional interval (loc. 10, Fig. 1b). Southeast of the Laswell thrust, this same transitional interval displays no mesoscopic deformation and consists of thick-bedded dolomite interbedded with red siltstone and sandstone (loc. 14, Fig. 1b).

Deformation southeast of the Laswell thrust consists

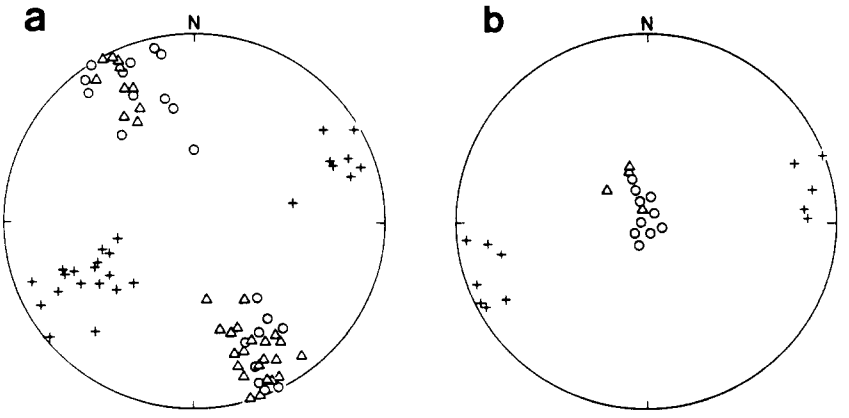

Fig. 7. Orientation data from zone of refolding near Max Meadows thrust, loc. 9 (Fig. 1b). (a) Crosses, first-phase fold axes (26); circles, poles to axial surfaces (21); and triangles, poles to cleavage (22). (b) Crosses, second-phase fold axes (12); circles, poles to axial surfaces (10); and triangles, poles to cleavage (4).

of macroscopic, upright, gentle to open folds alternating with SE-dipping thrusts (Stose & Stose 1957). The general lack of mesoscopic structures, cleavage, and veins in the Rome Formation contrasts with the presence of these features in the Max Meadows sheet. On the basis of these structural and stratigraphic differences, sedimentary strata southeast of the Laswell and Hiwassee thrusts are considered part of the Blue Ridge sheet.

FOLD-FAULT RELATIONS AND CHRONOLOGY

The continuous transition between upright and inclined folds, lack of structural overprinting within outcrops displaying this transition (e.g. Fig. 5), and similarity of tectonic foliations in both domains indicate that the two fold groups belong to a single generation. Some structures, including rare SE-facing folds (loc. 12, Fig. 1b), may have been reoriented by large-scale refolding, but this mechanism cannot account for all variations in fold orientation. Furthermore, refolding fails to explain the observed correlation between interlimb angle and axial plane dip (Fig. 4), as well as the high degree of veining, brecciation, faulting, and boudinage characteristic only of inclined fold zones. Variation of cleavage and fold axial surface attitude must, therefore, reflect strain distribution during generation of these structures. Throughout the remainder of the paper, these structures are referred to as first-phase.

Localization of inclined fold domains near the Max Meadows and various minor thrust faults (locs. 4–10, Fig. 1b) suggests a genetic link between faulting and inclined first-phase fold development. However, truncation of mesoscopic fold axis trends along the Max Meadows, Blue Ridge, and inferred thrusts implies that part of the movement on these faults postdates folding within the thrust sheet. Though incipient brecciation appears related to progressive strain on isoclinal fold limbs (Fig. 6f), clasts within breccias often display microfolds with an axial-plane foliation similar to first-phase fabrics (Gibson 1983). Faulting and brecciation, therefore, probably began during the later stages of folding and largely postdate establishment of the structural trends within the thrust sheet.

Second-generation structures typically occur in association with faults and probably developed in response to fault movement (cf. Schmid 1975, Bruhn 1979). Small scale features, including crenulations in breccia clasts (Gibson 1983), appear to reflect localized strain within or adjacent to thrust zones.

There is no compelling evidence to indicate that development of first-generation folds, faults, and second-generation structures were separated by a significant time gap. Rather, they appear to represent a successive chronological sequence in which faults evolved progressively from zones of inclined, first-phase folds, with second-generation structures reflecting movement along these faults (cf. Bruhn & Dalziel 1977). This chronology is interpreted as a transition from ductile (folding and cleavage development) to brittle (faulting) deformation within the Max Meadows thrust sheet. The distinction between these two types of deformation is based on observations at the meso- and macroscopic scales. Alternatively, the transition may be viewed in terms of changing deformation mechanisms and localization of strains into progressively narrower zones.

PHYSICAL CONDITIONS DURING DEFORMATION

Physical parameters, including temperature and pressure, affect the mechanical behavior of geologic materials during deformation (Handin *et al.* 1963, Paterson 1978). These variables must be considered in any analysis of a ductile-to-brittle transition. In the absence of metamorphic index minerals necessary to quantify temperature and pressure, foliation and vein morphology are used as qualitative indicators of physical conditions during the course of deformation (cf. Gray 1981, Beach & Jack 1982).

Foliations

First phase foliations consist of spaced to continuous (Powell 1979), white mica + chlorite fabrics in mudstone (Figs. 8a & b) and spaced, phyllosilicate + quartz-rich seams in microcrystalline dolomite. Siltstones, where cleaved, contain spaced, rough, disjunctive, opaque folia or a crude crenulation of a primary detrital mica fabric. Though intracrystalline strain is minor in both quartz (undulose extinction, deformation lamellae) and dolomite (undulose extinction, minor twinning), mineral grains show strong dimensional alignment adjacent to spaced cleavage domains. Thinned or truncated veins and bedding laminae indicate that dissolution of quartz and dolomite was an important deformation mechanism (Durney 1972, Groshong 1975, Beach 1979). Mica beards (Fig. 8c), detrital-shaped quartz grains in samples with continuous fabrics (Fig. 8a), and strong phyllosilicate alignment in lithons between spaced cleavage domains (Fig. 8b) indicate that phyllosilicate recrystallization/growth also occurred during cleavage development.

Second-generation crenulation cleavages are zonal to discrete (Gray 1979) and often occur in conjugate sets on opposite limbs of microfolds. Along boundaries between cleavage domains and lithons, the pre-existing fabric is deflected continuously into parallelism with the new cleavage and shows no evidence of phyllosilicate recrystallization (Fig. 8d) (cf. Weber 1981). Vein truncation is common and first phase lithons thin upon entering crenulation seams. These fabrics developed largely by dissolution accompanying microfolding (cf. Gray 1979). The lack of phyllosilicate recrystallization/growth involved in crenulation cleavage development suggests prevailing temperatures equivalent to, or lower than, those attained during first-phase ductile deformation (cf. Weber 1981).

Both foliation generations are enhanced by fibrous

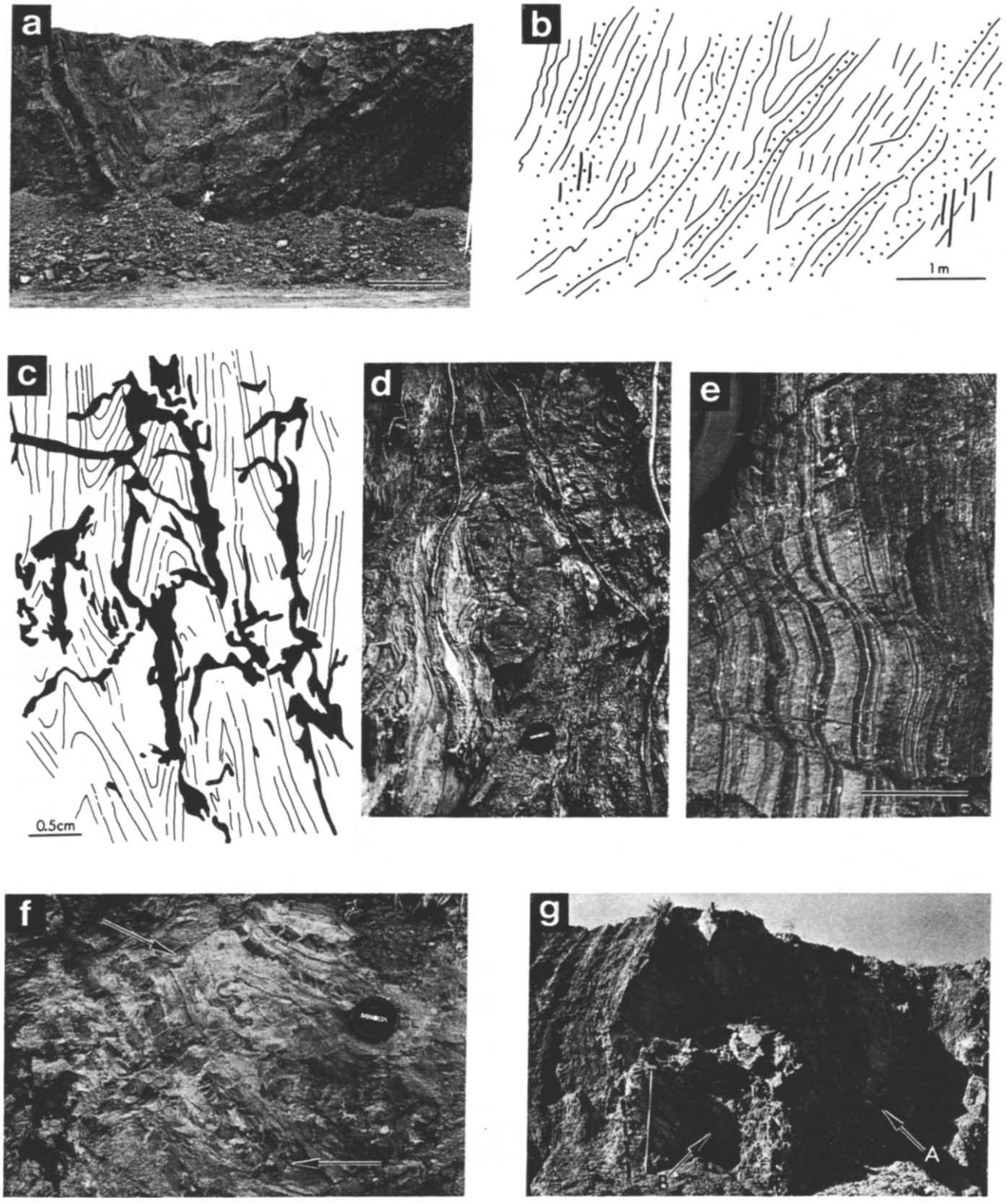

Fig. 6. Small scale structural elements. (a) Typical fold from upright fold domain, loc. 9 (Fig. 1b), scale bar = 3 m. (b) Isoclinally folded mudstones and closely spaced breccia zones (dotted), loc. 9 (Fig. 1b). (c) Folds in bedding of mudstone cut by post-first phase veins (black). Sketch of thin section from near Max Meadows thrust, loc. 5 (Fig. 1b). (d) Fold hinge isolated within strongly cleaved dolomite matrix, near Max Meadows thrust, loc. 5 (Fig. 1b), scale bar = 10 cm. (e) Asymmetric boudins in interlaminated mudstone and dolomite near Max Meadows thrust, loc. 8 (Fig. 1b), scale bar = 2 cm. (f) Tightly folded dolomite layers (hinges at arrows) showing attenuation and incipient brecciation on fold limbs, loc. 4 (Fig. 1b). (g) Coaxially refolded isocline adjacent to small fault (A, first-phase fold hinge; B, second-generation fold hinge); loc. 9 (Fig. 1b), staff height = 1.5 m.

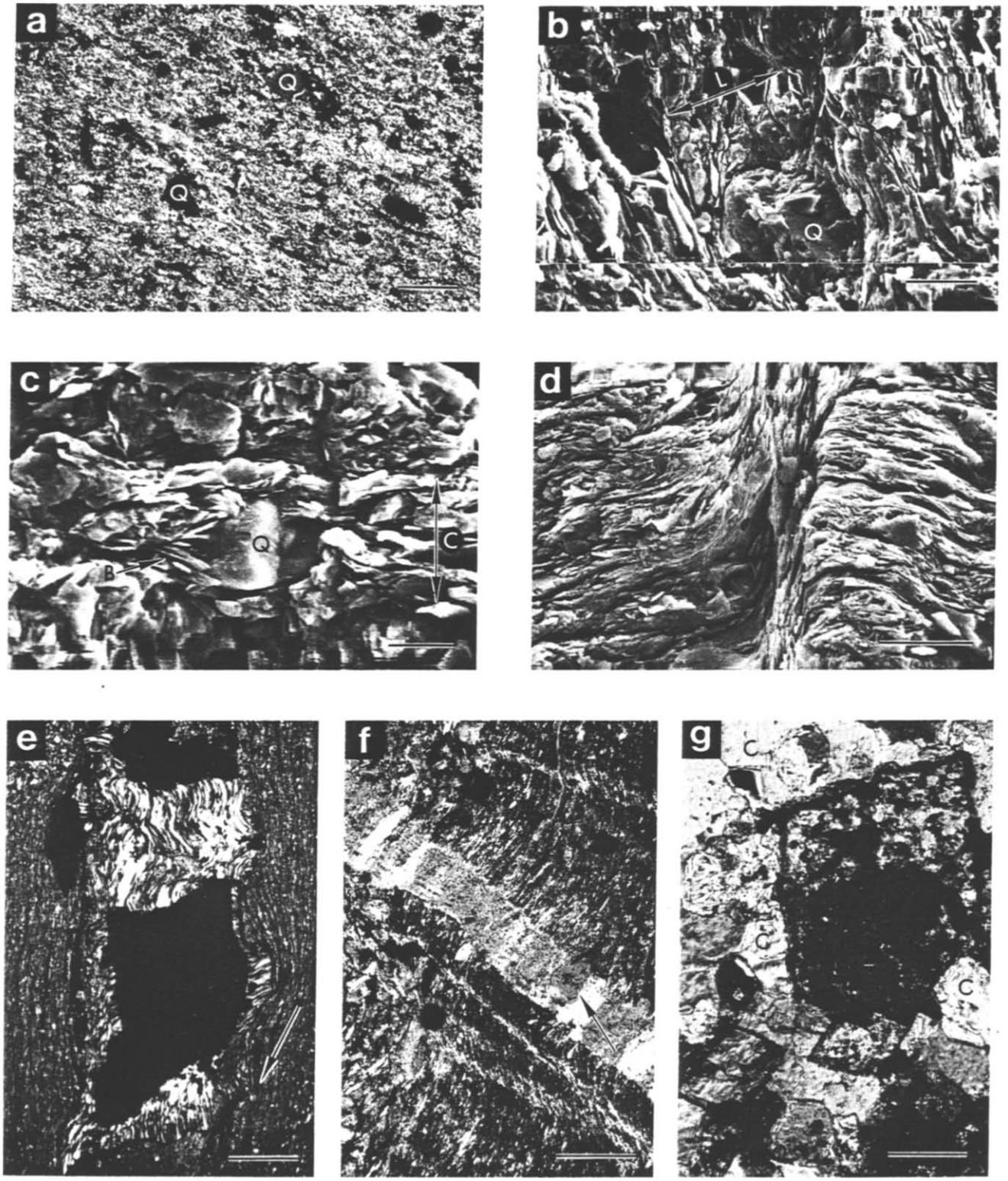

Fig. 8. Rome Formation microfabrics. (a) Detrital-shaped quartz grains (Q) within continuous first-phase fabric defined by white micas and elongate dolomite (crossed polars, scale bar = 100 μm). (b) Quartz grain (Q) and strong phyllosilicate alignment in lithon (L) between spaced cleavage domains in mudstone (SEM micrograph, scale bar = 10 μm). (c) Mica beard adjacent to quartz grain (Q) in spaced cleavage domain (C) of microcrystalline dolomite (SEM micrograph, scale bar = 5 μm). (d) SEM micrograph of second-generation crenulation cleavage (scale bar = 10 μm). (e) Quartz pressure fringe adjacent to pyrite grain (black); curved vertical fibers grew during first-phase cleavage development and subhorizontal fibers parallel weak second-generation crenulation (arrow) (crossed polars, scale bar = 0.5 mm). (f) Syn-first phase crack–seal quartz vein and second-generation crenulations in hematitic mudstone; note chlorite infilling between segments of extended detrital biotite (arrow) (partly crossed polars, scale bar = 100 μm). (g) Euhedral dolomite crystals preserved as limonitic outlines in mosaic of replacement calcite (C) in post-first phase vein (crossed polars, scale bar = 100 μm).

mineral growth in veins and pressure fringes (Fig. 8e). Curved quartz, chlorite, and carbonate fibers record rotational strain increments during first-phase foliation development (cf. Durney & Ramsay 1973), even in the absence of a second-generation fabric.

Veins

Veins are divisible into two types: systematic and non-systematic. Systematic veins occur at high angles to either bedding or cleavage and define convergent fans around fold closures (Fig. 9). Many are deformed or display ambiguous cross-cutting relationships with first-phase cleavage domains. Fractures contain ferroan calcite, ferroan dolomite, quartz, or chlorite with euhedral (Beach 1977), equant, fibrous (cf. Durney & Ramsay 1973), or crack–seal morphologies (Fig. 8f) (Ramsay 1980).

The geometric relationship between systematic veins, fold axes, and first-phase cleavage (Fig. 9) implies a genetic and temporal link between these features. Some syntectonic veins within the Max Meadows sheet record extension within the bedding plane and may reflect folding by tangential longitudinal strain (Ramsay 1967). Most fibrous mineral growth was, however, controlled by extension in the cleavage plane.

Non-systematic veins, associated with breccias and fault zones, occur as complex networks that cross-cut first-phase fold hinges or follow bedding and foliation planes (Fig. 6b). Euhedral, strained, ferroan dolomite crystals line fracture walls and a mosaic of unstrained, ferroan calcite occupies the center of the veins and locally replaces the dolomite (Fig. 8g).

Non-systematic arrays postdate systematic veins and first-phase structures. Euhedral crystals along vein margins suggest their origin as fluid-filled, hydraulic fractures (Beach 1977). Their distribution appears most consistent with dilation of the rock mass across inherently weak surfaces.

Most previous workers (e.g. Secor 1965, Phillips 1972, Beach 1977, Ramsay 1980, Beach & Jack 1982) have concluded that vein arrays develop by hydraulic fracturing and reflect fluid pressure conditions at the time of their generation. Systematic veins imply fluid pressures (P_f) in excess of only the minimum compressive stress (σ_3) (Etheridge 1983). Multidirectional dilation to form non-systematic vein arrays, however, suggests more nearly hydrostatic conditions ($P_f = \sigma_1 = \sigma_3 = \sigma_n$). Relative values of fluid pressure and principal stresses apparently changed from values of $\sigma_3 + T < P_f < \sigma_1 + T$ (T = tensile strength) during ductile deformation to $P_f = \sigma_n + T$ within future fault zones at the onset of brittle deformation.

DISCUSSION

Thrust sheets are characterized by localized high strain along the base and lower strains in the upper portions (Elliott 1976, Sanderson 1982, Wojtal 1982).

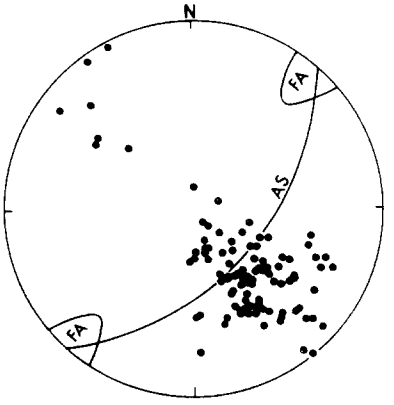

Fig. 9. Systematic vein (•), fold axis (*FA*), and axial surface (*AS*) orientations from inclined fold domain, loc. 4 (Fig. 1b) (n = 96 veins).

To accommodate basal sliding without production of large voids, a thrust sheet deforms internally by either whole-rock deformation (including folding and cleavage development) or sliding on discrete surfaces (e.g. faults or bedding planes), depending on physical conditions (Elliott 1976). Both mechanisms of internal deformation involve a large simple shear component (Elliott 1976, Wojtal 1982). These two end-member types of thrust sheet distortion may be viewed as ductile and brittle processes, respectively, and may be transitional into one another in some circumstances (Beach 1981, Ramsay *et al.* 1983, Mitra *et al.* 1984). The ductile-to-brittle transition observed in the Max Meadows sheet is thought to reflect changing physical conditions during deformation related to thrust sheet emplacement.

Development of first-phase structures

Rotational strains during first-phase ductile deformation are implied by the variable orientation and intensity of structures (Sanderson 1979) and the occurrence of curved mineral fibers in pressure fringes (Durney & Ramsay 1973). Since fold tightening and reorientation occurs continuously within single layers in individual outcrops, a shear zone model is applicable (Ramsay & Graham 1970, Sanderson 1979, 1982). Though most commonly applied to deformation in crystalline terranes (Bryant & Reed 1969, Ramsay & Graham 1970, Escher & Watterson 1974, Mitra & Elliott 1979), the effects of simple shear have been recognized in several low-grade, sedimentary provinces (Sanderson 1979, Bruhn 1979, Tanner & Macdonald 1982, Bosworth & Vollmer 1981, Ramsay *et al.* 1983). Features, including (1) consistent fold facing across a large area, (2) systematic strain increase in one direction, (3) correlation between fold tightness and axial-plane attitude, (4) non-cylindrical folds and (5) variable fold axis orientation with respect to stretching lineation, characterize regions deformed in simple shear. Several of these features (1, 3, 4) are observed in the Max Meadows sheet. Strain magnitude, indicated by fold tightness and boudinage, shows no systematic variation across the thrust sheet (note locations of inclined fold domains in Fig. 1b). Rather, highest

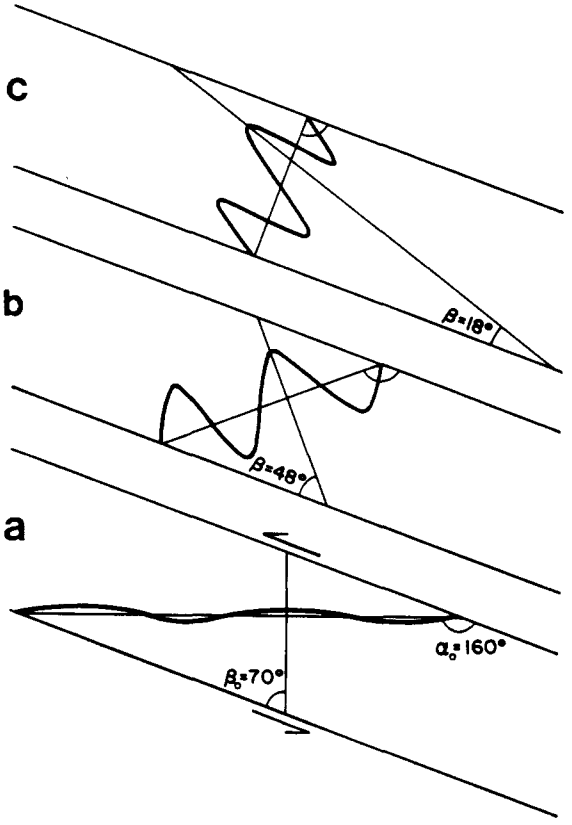

Fig. 10. Idealized progressive (a–c) folding of a layer undergoing simple shear along a 20° dipping zone with reverse movement (after Ghosh 1966, Sanderson 1979).

strains are localized in many, often mesoscopic, zones along which thrust faults later developed.

Rotational and distortional components of simple shear result in changes in the orientation and intensity of structural elements. The degree of this modification may be used to estimate shear strain magnitude (Ramsay 1967, Sanderson 1979). Folds developing in simple shear nucleate with axial surfaces at a high angle to layering and not necessarily parallel to the XY plane of the total strain ellipsoid (Fig. 10a) (Ghosh 1966, Manz & Wickham 1978). Further shearing causes rotation of bedding planes according to the relation

$$\cot \alpha = \cot \alpha_0 + \gamma, \quad (1)$$

where γ = shear strain and α_0 and α are initial and final angles between the shear plane and bedding (Fig. 10a) (Ramsay 1967, Sanderson 1979). For a known shear strain and initial orientation of layering with respect to the shear plane, the elongation of a line (λ = (final length/initial length)^2) may be calculated from

$$\lambda = 1 + \gamma^2 \sin^2 \alpha_0 + \gamma \sin 2\alpha_0 \quad (2)$$

(Sanderson 1979).

An estimate of the shear strain recorded in inclined fold domains of the Max Meadows sheet may be made using a modification of Sanderson's (1979) method. This treatment assumes that inclined and upright folds developed directly from undeformed strata by heterogeneous simple shear without volume loss. Three parameters, shear plane orientation, original bedding attitude, and initial axial surface orientation, must be determined to establish the original angles between shear plane and bedding (α_0) and shear plane and axial surfaces (β_0) (Fig. 10a) (Sanderson 1979). Longitudinal strains, indicated qualitatively by fold tightness, are lowest within upright fold domains of the Max Meadows sheet. Assuming that these folds with vertical axial surfaces also formed at lowest shear strains, bedding is inferred to have been horizontal prior to deformation (Ghosh 1966, Manz & Wickham 1978). Consequently, shear zone dip = 180 − α_0 (Fig. 10a).

In view of the regional structural framework (e.g. Harris & Bayer 1979), any shear zone associated with compression in the Southern Appalachians should dip moderately to gently SE. Since fold axial surfaces in inclined domains generally dip 30° SE and folds define a gently NW-dipping enveloping surface, the shear plane dip cannot exceed 30° SE (α_0 = 150°).

Substituting α_0 = 150° and longitudinal strain in inclined domains (λ_{incl}) = 0.25 (Table 1) into equation (2) yields a value of γ = 1.6. Since (180 − α_0) = 30° is a maximum, this value of γ must be considered a minimum.

Linear features, such as fold hinges, rotate toward the transport direction in zones undergoing simple shear (Bryant & Reed 1969, Escher & Watterson 1974). The degree of fold axis rotation places constraints on shear zone orientation and the maximum shear strain value (Skjernaa 1980). Fold hinges within the Max Meadows sheet show only minor reorientation within the axial surface in inclined fold domains (Fig. 3c). Skjernaa's (1980) mathematical models show that sub-horizontal lineations, trending at a high angle to a horizontal shear direction, begin significant rotation at γ = 3. The pattern illustrated by Skjernaa (1980, fig. 5c) resembles the fold axis distribution from inclined-fold zones in the study area (Fig. 3c). Taking γ = 3 as a maximum for fold generation in these zones, equation (2) yields a shear zone dip of 24° SE (α_0 = 156°).

These calculations indicate that shear strains up to γ = 3 were necessary to create structures in the inclined-fold domains within the Max Meadows sheet. The calculated shear plane dip of 24–30° SE should be considered a maximum since strain related to cleavage development was not incorporated in the λ_{incl} term of equation (2); the actual shear plane was probably more gently dipping. Shear strains were too low to cause significant fold axis reorientation or development of a prominent stretching

Table 1. Longitudinal strain data from inclined fold domains

Location (see Fig. 1b)	Undeformed bed length (m)	Deformed bed length (m)	λ
4	18.1	7.4	0.16
4	23.2	12.8	0.24
4	17.2	7.4	0.18
4	16.0	10.0	0.42
4	31.6	16.6	0.28
7	7.0	3.6	0.26
7	7.2	3.4	0.22

Average λ_{incl} = 0.25

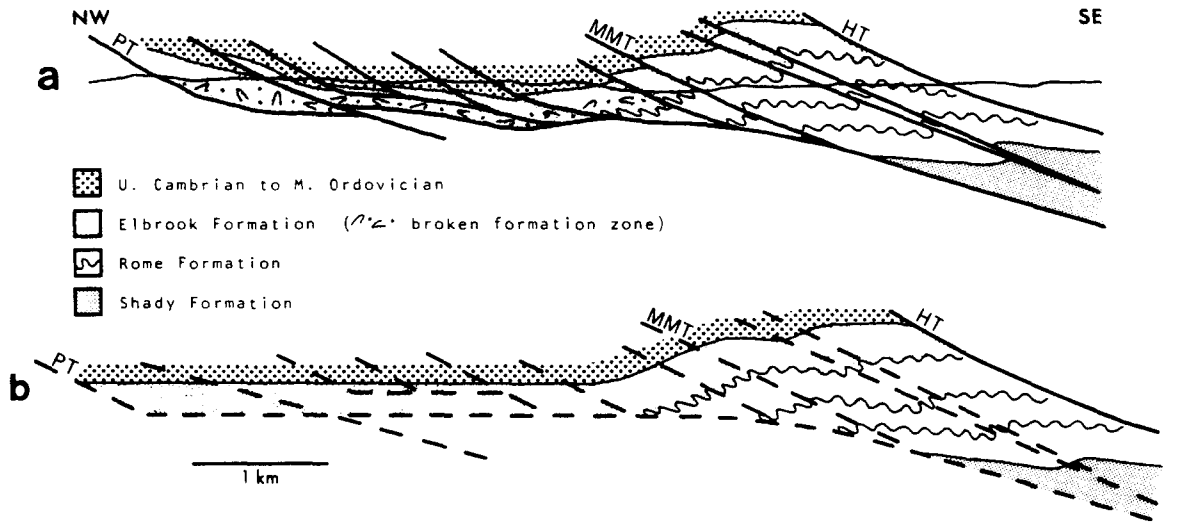

Fig. 11. Cross section of Pulaski thrust sheet after (a) and before (b) brittle phase of deformation. Mesoscopic fold geometry in the Rome Formation is shown schematically.

lineation (cf. Sanderson 1979, Bruhn 1979). Greatest shear strains, and therefore inclined folds, are localized in stratigraphic intervals dominated by mudstone and argillaceous carbonate. Lack of axial surface reorientation in more competent lithologies of upright fold domains, however, reflects relatively low shear strains.

The transition to brittle behavior

Field and petrographic observations demonstrate that faulting and brecciation largely postdate first-phase folding. Localization of faults in zones of inclined folds with rare axial surface truncation suggests that these brittle features developed progressively from ductile structures at points of highest shear strain in a similarly oriented stress field (cf. Beach 1981, Ramsay *et al.* 1983).

The ductile-to-brittle transition was, along incipient fault zones, accompanied by an increasing ratio of fluid pressure to maximum confining stress (σ_n). Fluid pressures affect the mechanical behavior of geologic materials such that increasing $P_f : \sigma_n$ results in lowering of the differential effective stress necessary for fracturing (Hubbert & Rubey 1959, Secor 1965, Phillips 1972) and, therefore, decreasing ductility (Handin *et al.* 1963, Paterson 1978). Increasing $P_f : \sigma_n$ was probably significant during brecciation and fault initiation in the Max Meadows sheet. The localization of hydrostatic overpressures ($P_f = \sigma_n + T$) to inclined fold domains and incipient fault zones may be partially lithologically controlled (cf. Suppe & Wittke 1977). Northwest of the Max Meadows thrust, intense fracturing is restricted to argillaceous carbonates in the lower Elbrook Formation, and Schultz (1983) attributes this to hydraulic fracturing in response to fluid confinement by thin shaly layers. Similarly, interlaminated mudstone, microcrystalline dolomite, and argillaceous carbonate typical of inclined fold zones may have been less permeable than coarser grained, siliciclastic strata of upright fold domains.

Cleavage fabrics suggest that second-generation, fault-related cleavages developed at lower temperatures than first-phase foliations. Maximum temperatures of 200–300°C resulted from burial metamorphism (Epstein *et al.* 1977) and were apparently attained during first-phase folding. Burial metamorphic temperatures in the 200–300°C range can only be attained at depths of 5–11 km assuming an average geothermal gradient of 25–35°C/km (cf. table 1 in Suppe & Wittke 1977, Orkan & Voight 1983) and surface temperature of 20°C. Burial beneath the normal stratigraphic section (<5 km thick) above the Rome Formation (Schultz in press) is insufficient to account for these temperatures. Most likely, rocks of the structurally overlying Blue Ridge thrust sheet were in place above the Pulaski sheet during first-phase deformation. Decreasing temperature between first- and second-generation cleavage development may reflect unroofing of the Blue Ridge/Pulaski sheet and have contributed to decreased ductility during deformation.

Model

Removal of displacement along faults within the Pulaski sheet shows the inferred structural configuration after only ductile folding and cleavage development (Figs. 11a & b). In these diagrams, constructed by maintaining constant length along the base of the Upper Cambrian and the Shady–Rome contact, ductile shear zones are assumed to dip 20° SE. The sole of the Pulaski sheet is comprised of a zone of intense deformation, including the rocks in the Max Meadows sheet and the zone of broken formation northwest of the Max Meadows thrust (Schultz 1983, in press). The continuity of these two structural domains in the restored section (Fig. 11b) suggests that they may have been deformed by similar processes. Rocks in the broken formation probably underwent a history of folding followed by brecciation similar to, though more complex than, that experienced by the rocks of the Max Meadows sheet.

Several workers have shown that shear strains decrease upward from the base of a thrust sheet (Elliott 1976, Sanderson 1982, Wojtal 1982). In the Pulaski sheet, this decrease is not gradual but occurs abruptly

across lithologic boundaries which acted as detachments (cf. Harris & Milici 1977). Shear-related deformation is restricted to argillaceous strata structurally below the competent upper Elbrook dolomite and Shady Formation or Chilhowee Group of the Blue Ridge sheet. Schultz (1983) demonstrated that argillaceous horizons in the middle Elbrook behaved as detachments separating the broken formation from the less deformed upper portion of the sheet. After emplacement of the Blue Ridge sheet, the Blue Ridge/Hiwassee/Laswell thrust system probably also acted as a detachment allowing localization of shear strains in structurally underlying, incompetent Rome strata. As a result, Rome sedimentary rocks preserved above the Shady dolomite within the Laswell thrust sheet do not exhibit significant effects of shear deformation.

Ductile deformation, dominated by folding and cleavage development, evolved progressively into sliding along narrow fault zones. This ductile-to-brittle transition probably reflects both decreasing temperatures and increasing $P_f:\sigma_n$ ratios within developing fault zones. Unroofing of the thrust sheet during emplacement may have resulted in decreasing temperatures and confining pressures (cf. Mitra *et al.* 1984). Decreasing σ_n, combined with constant or increasing P_f in low permeability strata along the base of the sheet led to fracturing and brecciation. Brittle deformation involved imbrication of the thrust sheet and incorporation of numerous large horses, derived from Cambrian to Mississippian strata of the footwall ramp.

Deformation in the Appalachian fold-and-thrust belt has traditionally been attributed to late Paleozoic ("Alleghenian") orogenesis (Perry 1978). However, recent workers initially interpreted polyphase structures in the Pulaski sheet to reflect both Alleghenian and possible pre-Alleghenian deformation (Bartholomew & Lowry 1979, Bartholomew *et al.* 1980). The data presented in this paper, coupled with that of Bartholomew *et al.* (1982) and Schultz (1983, in press), are most consistent with progressive development of these structures during protracted, late Paleozoic thrust sheet emplacement.

Acknowledgements—Financial support for this project was provided in the form of a Teaching Assistantship to R. G. Gibson from Virginia Polytechnic Institute and grants from Sigma Xi (the Scientific Research Society of North America) and the American Association of Petroleum Geologists. Additional funds were supplied by N.S.F. grant EAR-81-20948 to D. R. Gray. We would like to thank K. A. Eriksson, D. R. Wones, L. Glover III, C. Simpson, G. Mitra, S. Cox and D. J. Sanderson for reading the manuscript and suggesting numerous improvements. Thanks also to Lynn Sharp for assistance with photography, Sharon Chiang and her staff for drafting, Carl Price for SEM photography, and Janet Schweitzer for typing and reviewing parts of the manuscript.

REFERENCES

Bally, A. W., Gordy, P. L. & Stewart, G. A. 1966. Structure, seismic data and orogenic evolution of the southern Canadian Rockies. *Bull. Can. Petrol. Geol.* **14**, 337–381.

Bartholomew, M. J. 1979. Thrusting component of shortening and a model for thrust fault development at the Central/Southern Appalachian junction. *Abs. with Prog. Geol. Soc. Am.* **11**, 384–385.

Bartholomew, M. J. & Lowry, W. D. 1979. Geology of the Blacksburg Quadrangle, Virginia. *Virginia Div. Min. Res. Publ.* **14**, 1 sheet.

Bartholomew, M. J., Milici, R. C. & Schultz, A. P. 1980. Geologic structure and hydrocarbon potential along the Saltville and Pulaski thrusts in southwestern Virginia and northeastern Tennessee. *Virginia Div. Min. Res. Publ.* **23**, 6 sheets.

Bartholomew, M. J., Schultz, A. P., Henika, W. S. & Gathright, T. M. II. 1982. Geology of the Blue Ridge and Valley and Ridge at the junction of the Central and Southern Appalachians. In: *Central Appalachian Geology, Northeastern-Southeastern sections combined Mtg. geol. Soc. Am.* Field Trip Guidebook, 121–170.

Beach, A. 1977. Vein arrays, hydraulic fractures and pressure solution structures in a deformed flysch sequence, S.W. England. *Tectonophysics* **40**, 201–226.

Beach, A. 1979. Pressure solution as a metamorphic process in deformed terrigenous sedimentary rocks. *Lithos* **12**, 51–58.

Beach, A. 1981. Some observations on the development of thrust faults in the Ultradauphinois Zone, French Alps. In: *Thrust and Nappe Tectonics* (edited by McClay, K. R. & Price, N. J.). Blackwell Science Publ., Oxford, England, 329–334.

Beach, A. & Jack, S. 1982. Syntectonic vein development in a thrust sheet from the External French Alps. *Tectonophysics* **81**, 67–84.

Bosworth, W. & Vollmer, F. W. 1981. Structures of the Medial Ordovician Flysch of Eastern New York: deformation of synorogenic deposits in an overthrust environment. *J. Geol.* **89**, 551–568.

Boyer, S. E. & Elliott, D. 1982. Thrust systems. *Bull. Am. Ass. Petrol. Geol.* **66**, 1196–1230.

Bruhn, R. L. 1979. Rock structures formed during back-arc basin deformation in the Andes of Tierra del Fuego. *Bull. geol. Soc. Am.* **90**, 998–1012.

Bruhn, R. L. & Dalziel, I. W. D. 1977. Destruction of the Early Cretaceous marginal basin in the Andes of Tierra del Fuego. In: *Island Arcs, Deep Sea Trenches, and Back-Arc Basins* (edited by Talwani, M. & Pitman, W. C. III). *Trans. Am. Geophys. Un.* Washington, D.C., 395–406.

Bryant, B. & Reed, J. C., Jr. 1969. Significance of lineation and minor folds near thrust faults in the southern Appalachians and Norwegian Caledonides. *Geol. Mag.* **106**, 412–429.

Cobbold, P. R., Cosgrove, J. W. & Summers, J. M. 1971. Development of internal structures in deformed anisotropic rocks. *Tectonophysics* **12**, 23–53.

Cook, F. A., Albaugh, D. S., Brown, L. D., Kaufman, S., Oliver, J. E. & Hatcher, R. D., Jr. 1979. Thin-skinned tectonics in the crystalline Southern Appalachians: COCORP seismic-reflection profiling of the Blue Ridge and Piedmont. *Geology* **7**, 563–567.

Cooper, B. N. 1939. Geology and Mineral Resources of the Draper Mountain area, Virginia. *Va. Geol. Survey Bull.* **55**, 1–98.

Cooper, B. N. 1970. The Max Meadows breccias; a reply. In: *Studies in Appalachian Geology—Central and Southern* (edited by Fisher, G. W., Pettijohn, F. J., Reed, J. C., Jr. & Weaver, K. N.). Wiley-Interscience, New York, 179–191.

Cooper, B. N. & Haff, J. C. 1940. Max Meadows fault breccia. *J. Geol.* **48**, 945–974.

DeSitter, L. H. & Zwart, H. J. 1960. Tectonic development in supra- and infra-structures of a mountain chain. *21st Int. geol. Cong., Copenhagen Report* **18**, 248–256.

Durney, D. W. 1972. Solution transfer, an important geologic deformation mechanism. *Nature, Lond.* **235**, 315–317.

Durney, D. W. & Ramsay, J. G. 1973. Incremental strains measured by syntectonic crystal growths. In: *Gravity and Tectonics* (edited by DeJong, K. A. & Scholten, R.). Wiley, New York, 67–96.

Elliott, D. 1976. The energy balance and deformation mechanisms of thrust sheets. *Phil. Trans. R. Soc.* **A283**, 289–312.

Epstein, A. G., Epstein, J. B. & Harris, L. D. 1977. Conodont color alteration—an index to organic metamorphism. *Prof. Pap. U.S. geol. Surv.* **995**.

Escher, A. & Watterson, J. 1974. Stretching fabrics, folds and crustal shortening. *Tectonophysics* **22**, 223–231.

Etheridge, M. A. 1983. Differential stress magnitudes during regional deformation and metamorphism: upper bound imposed by tensile fracturing. *Geology* **11**, 231–234.

Fyson, W. K. 1971. Fold attitudes in metamorphic rocks. *Am. J. Sci.* **270**, 373–382.

Ghosh, S. K. 1966. Experimental tests of buckling folds in relation to strain ellipsoid in simple shear deformations. *Tectonophysics* **3**, 169–185.

Gibson, R. G. 1983. Structural Evolution of the Max Meadows thrust sheet, Southwest Virginia. Unpublished M.S. thesis, Virginia Polytechnic Institute & State University.

Gray, D. R. 1979. Microstructure of crenulation cleavages: an indicator of cleavage origin. *Am. J. Sci.* **279**, 97–128.

Gray, D. R. 1981. Compound tectonic fabrics in singly folded rocks from southwest Virginia, U.S.A. *Tectonophysics* **78**, 229–248.

Groshong, R. H. 1975. "Slip" cleavage caused by pressure solution in a buckle fold. *Geology* **3**, 411–413.

Gwinn, V. E. 1964. Thin-skinned tectonics in the Plateau and northwestern Valley and Ridge provinces of the Central Appalachians. *Bull. geol. Soc. Am.* **75**, 863–899.

Handin, J., Hagar, R. V., Friedman, M. & Feather, J. N. 1963. Experimental deformation of sedimentary rocks under confining pressure: pore pressure tests. *Bull. Am. Ass. Petrol. Geol.* **47**, 717–755.

Harris, L. D. & Bayer, K. C. 1979. Sequential development of the Appalachian orogen above a master decollement—a hypothesis. *Geology* **7**, 568–572.

Harris, L. D. & Milici, R. C. 1977. Characteristics of thin-skinned style of deformation in the Southern Appalachians, and potential hydrocarbon traps. *Prof. Pap. U.S. geol. Surv.* **1018**.

Hubbert, M. K. & Rubey, W. W. 1959. Role of fluid pressure in mechanics of overthrust faulting—I. *Bull. geol. Soc. Am.* **70**, 115–166.

Manz, R. & Wickham, J. 1978. Experimental analysis of folding in simple shear. *Tectonophysics* **44**, 79–90.

McDowell, R. C. 1968. Structural geology of the Macks Mountain area, Virginia. Unpublished Ph.D. thesis, Virginia Polytechnic Institute & State University.

Mitra, G. & Elliott, D. 1979. Deformation of basement in the Blue Ridge and the development of the South Mountain cleavage. In: *The Caledonides in the USA* (edited by Wones, D. R.). *Virginia Polytechnic Institute Dept. of Geol. Sci. Mem.* **2**, 307–312.

Mitra, G., Yonkee, W. A. & Gentry, D. J. 1984. Solution cleavage and its relationships to major structures in the Idaho–Utah–Wyoming thrust belt. *Geology* **12**, 354–358.

Orkan, N. I. & Voight, B. 1983. Fracture geometry and vein mineral paleothermometry-barometry from fluid inclusions, Valley and Ridge Province, Pennsylvania. *Abs. with Prog. geol. Soc. Am.* **15**, 656.

Paterson, M. S. 1978. *Experimental Rock Deformation—the Brittle Field*. Springer, Berlin.

Perry, W. J. 1978. Sequential deformation in the Central Appalachians. *Am. J. Sci.* **278**, 518–542.

Phillips, W. J. 1972. Hydraulic fracturing and mineralization. *J. Geol. Soc. Lond.* **128**, 337–359.

Powell, C. McA. 1979. A morphological classification of rock cleavage. *Tectonophysics* **58**, 21–34.

Ramsay, J. G. 1967. *Folding and Fracturing of Rocks*. McGraw-Hill, New York.

Ramsay, J. G. 1980. The crack–seal mechanism of rock deformation. *Nature, Lond.* **284**, 135–139.

Ramsay, J. G., Casey, M. & Kligfield, R. 1983. Role of shear in development of Helvetic fold-thrust belt of Switzerland. *Geology* **11**, 439–442.

Ramsay, J. G. & Graham, R. H. 1970. Strain variation in shear belts. *Can. J. Earth Sci.* **7**, 786–813.

Sanderson, D. J. 1979. The transition from upright to recumbent folding in the Variscan fold belt of southwest England: a model based on the kinematics of simple shear. *J. Struct. Geol.* **1**, 171–180.

Sanderson, D. J. 1982. Models of strain variation in nappes and thrust sheets: a review. *Tectonophysics* **88**, 201–233.

Schmid, S. M. 1975. The Glarus Overthrust: field evidence and mechanical model. *Eclog. geol. Helv.* **68**, 247–280.

Schultz, A. P. 1979. Deformation associated with Pulaski overthrusting in the Price Mountain and East Radford Windows, Montgomery County, southwest Virginia. Unpublished M.S. thesis, Virginia Polytechnic Institute & State University.

Schultz, A. P. 1983. Broken formations of the Pulaski thrust sheet near Pulaski, Virginia. Unpublished Ph.D. thesis, Virginia Polytechnic Institute & State University.

Schultz, A. P. in press. Broken formations of the Pulaski thrust sheet near Pulaski, Virginia. *Virginia Polytechnic Institute Dept. of Geol. Sci. Memoir* **3**.

Schweitzer, J. 1984. Cleavage development in dolomite, Elbrook Formation, Pulaski thrust sheet, Southwest Virginia. Unpublished M.S. thesis, Virginia Polytechnic Institute & State University.

Secor, D. T. 1965. Role of fluid pressure in jointing. *Am. J. Sci.* **263**, 633–646.

Skjernaa, L. 1980. Rotation and deformation of randomly oriented planar and linear structures in progressive simple shear. *J. Struct. Geol.* **2**, 101–109.

Spigai, J. J. 1963. A study of the Rome Formation in the Valley and Ridge Province of East Tennessee. Unpublished M.S. thesis, University of Tennessee.

Stose, A. J. & Stose, G. W. 1957. Geology and mineral resources of the Gossan Lead District and adjacent areas in Virginia. *Va. Div. Min. Res. Bull.* **72**, 1–223.

Suppe, J. 1980. A retrodeformable cross section of northern Taiwan. *Proc. geol. Soc. China* **23**, 46–55.

Suppe, J. & Wittke, J. H. 1977. Abnormal pore-fluid pressures in relation to stratigraphy and structure in the active fold-and-thrust belt of northwestern Taiwan. *Petrol. Geol. Taiwan* **14**, 11–24.

Tanner, P. W. G. & MacDonald, D. I. M. 1982. Models for deposition and simple shear deformation of a turbidite sequence in the South Georgia portion of the Southern Andes back-arc basin. *J. geol. Soc. Lond.* **139**, 739–754.

Weber, K. 1981. Kinematic and metamorphic aspects of cleavage formation in very low-grade metamorphic slates. *Tectonophysics* **78**, 291–306.

Wells, P. D. 1975. A seismic reflection and refraction study near the Blue Ridge thrust in Virginia. Unpublished M.S. thesis, Virginia Polytechnic Institute & State University.

Wojtal, S. F. 1982. Finite deformation in thrust sheets and their material properties. Unpublished Ph.D. thesis, Johns Hopkins University.